

Y. Tasa

A Time-Domain Technique for Measurement of the Dielectric Properties of Biological Substances

2421

MAGDY F. ISKANDER AND STANISLAW S. STUCHLY

Abstract—A time-domain (transient) method for (broad-band) measurement of the dielectric properties of biological substances is described. Theoretical analysis of the time dependence of the reflection coefficient following application of a step voltage to a shunt capacitor located at the end of a transmission line and filled with a very small amount of the dielectric showing the Debye dispersion is given. Analysis and calculations of the overall uncertainty of permittivity measurements as well as experimental results are presented and limitations of the method discussed.

INTRODUCTION

INVESTIGATIONS of the dielectric properties of biological substances and their frequency and temperature dependence give very valuable information about the state of water (free or bound), molecular structure, and hydration processes that are of primary importance in biochemistry and biophysics [1].

Currently used methods both in frequency and time domain, although highly refined and accurate, do not meet all the requirements imposed by experiments with biological substances [1]. In particular, a relatively large sample is required to fill a test capacitor or a section of a coaxial line [2], [3], especially when substances with long relaxation times are measured [4].

In the proposed technique a small shunt capacitor terminating a coaxial line section is used as a sample holder [Fig. 1(a)]. An equivalent circuit of the sample holder is shown in Fig. 1(b), where $\epsilon_r^*(\omega)$ is the relative complex permittivity.¹ The frequency behavior of the substance filling the test capacitor can be calculated from the time response of the reflected wave to an incident step voltage applied to the capacitor. The time dependence of the reflected wave is closely related to the dispersion mechanism of the dielectric. The frequency behavior of $\epsilon_r^*(\omega)$ can be obtained by the Fourier transform of the reflected wave.

THEORY

When a time-domain reflectometer (TDR) is used, a very fast rise (subnanosecond) voltage step is generated, while both

Manuscript received June 15, 1972; revised June 29, 1972. This research was supported by the National Research Council of Canada and the Faculty of Graduate Studies of the University of Manitoba.

The authors are with the University of Manitoba, Winnipeg, Man., Canada.

¹This assumption is not absolutely correct because of fringing field effects, but it is justified as a first-order approximation.

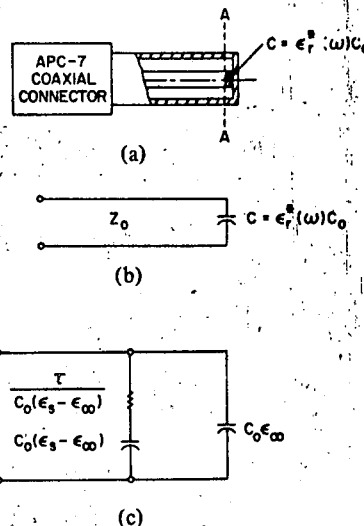


Fig. 1. (a) APC-7 Coaxial sample holder and (b) its equivalent circuit. (c) Equivalent circuit for the sample holder filled with a dielectric showing the Debye dispersion.

incident and reflected waves are picked up by a high-impedance sampler and displayed on the screen of a broad-band sampling oscilloscope [4]. The deflection of the oscilloscope trace is proportional to the algebraic sum of the incident and reflected waves.

Assuming the amplitude of the incident wave equal to unity, the sum of the incident and reflected waves is equal to $f(t)$ and $f(t) = 1$ for $t < 0$ and $f(t) \neq 1$ for $t > 0$. From transmission line theory, the reflection coefficient for a transmission line terminated by a load impedance $Z_L(p) = 1/pC(p)$ is

$$\rho(p) = \frac{1 - Z_0 p C(p)}{1 + Z_0 p C(p)} \quad (1)$$

where $C(p)$ is the capacitance of the capacitor terminating the transmission line as in Fig. 1, while $p = j\omega$ and ω is the angular frequency. When the capacitor is filled with the test dielectric $C(p) = C_0 \epsilon_r^*(p)$, where C_0 is the capacitance of the air-filled capacitor, then the reflection coefficient is

$$\rho(p) = \frac{1 - p C_0 Z_0 \epsilon_r^*(p)}{1 + p C_0 Z_0 \epsilon_r^*(p)} \quad (2)$$

From (2) the frequency dependence of the reflection coefficient can be obtained by substituting the specific function $\epsilon_r^*(p)$ representing a particular mechanism of dispersion.

For the dielectrics showing the Debye dispersion

$$\epsilon_r^*(p) = \epsilon_\infty + \frac{(\epsilon_s - \epsilon_\infty)}{1 + p\tau} \quad (3)$$

where ϵ_s and ϵ_∞ are the dielectric constants at frequencies very low and very high in respect to the relaxation frequency, respectively, and τ is the relaxation time. Substituting (3) into (2) and putting

$$A = \tau - C_0 Z_0 \epsilon_s,$$

$$B = \frac{1}{(C_0 Z_0 \epsilon_\infty \tau)}$$

and

$$\epsilon_r'(\omega) = \frac{2 |\rho(\omega)| \sin \theta(\omega)}{\omega C_0 Z_0 [(|\rho(\omega)| \cos \theta(\omega) + 1)^2 + |\rho(\omega)|^2 \sin^2 \theta(\omega)]} \quad (8)$$

$$\epsilon_r''(\omega) = \frac{(1 - |\rho(\omega)|^2)}{\omega C_0 Z_0 [(|\rho(\omega)| \cos \theta(\omega) + 1)^2 + |\rho(\omega)|^2 \sin^2 \theta(\omega)]} \quad (9)$$

$$C = \tau + C_0 Z_0 \epsilon_s,$$

(2) can be written in the form

$$\rho(p) = -\frac{p^2 - ABp - B}{p^2 + CBp + B} \quad (4)$$

System response to a step-function excitation is

$$\Gamma(p) = \frac{\rho(p)}{p},$$

hence

$$\begin{aligned} \Gamma(p) &= -\frac{1}{p} \left(\frac{p^2 - ABp - B}{p^2 + CBp + B} \right) \\ &= -\left(\frac{p}{(p+a)(p+b)} - \frac{AB}{(p+a)(p+b)} - \frac{B}{p(p+a)(p+b)} \right) \quad (5) \end{aligned}$$

where a and b are the real negative roots² of the equation

$$p^2 + CBp + B = (p+a)(p+b).$$

System response on the oscilloscope screen, which is a sum of the incident and reflected waves, can be obtained by the inverse Laplace transform of the elements of (5)

$$\begin{aligned} f(t) = 1 + \Gamma(t) &= 2 - e^{-at} \left(\frac{a^2 + aAB - B}{a(a-b)} \right) \\ &\quad + e^{-bt} \left(\frac{b^2 + bAB - B}{b(a-b)} \right). \quad (6) \end{aligned}$$

A similar expression can be obtained also for the dielectrics showing the Debye dispersion with distributed relaxation times [5].

²It can be shown that for real dielectrics $0 < \epsilon_\infty < \epsilon_s$ always holds, so that $(CB)^2/4 - B > 0$ and the roots are real.

System response given by (6) may be used for checking the experimental data and necessary corrections can be easily provided, e.g., corrections for finite rise time of the system [4]. In addition to this, (6) may also be used to calculate ϵ_s , ϵ_∞ , and τ for the test substance by fitting the experimental data with the predicted curve by the method of least squares.

The behavior of the systems described by (6) is represented by a simple equivalent circuit shown in Fig. 1(c) where

$$Y = j\omega C = j\omega C_0 \epsilon_r^*(\omega) = j\omega C_0 \epsilon_\infty + \frac{j\omega C_0 (\epsilon_s - \epsilon_\infty)}{1 + j\tau\omega} \quad (7)$$

In an alternative approach the relative permittivity $\epsilon_r^*(\omega)$ may be found directly by solving (2) for the real and imaginary parts of the relative permittivity.

The reflection coefficient $\rho(\omega)$ appearing in (8) and (9) could be calculated by a discrete Fourier transform directly from the digitized system response $f(t)$ displayed on the screen of a sampling oscilloscope [3]. This technique was used in this paper.

MEASUREMENT TECHNIQUES

In order to determine experimentally the frequency dependence of the reflection coefficient $\rho(\omega)$ the following measurement procedure has been adopted.

When the sample holder is short circuited at the plane $A - A$ in Fig. 1(a), the waveform displayed by the oscilloscope is $V_{sc}(t - t_0)$ where

$$t_0 = \frac{\text{distance between the sampler and } A - A}{\text{speed of light}}$$

and $V_{sc}(t - t_0) = -V_{in}(t - t_0)$ where V_{in} is the incident wave (Fig. 2). With the test sample between the plates of the capacitor, the displayed waveform will be

$$V_0(t) = V_{in}(t - 2t_0) + V_r(t - t_0) \quad (10)$$

and

$$V_r(t - t_0) = V_0(t) - V_{in}(t - 2t_0) = V_{in}(t - t_0) * \rho(t) \quad (11)$$

where V_r is the reflected wave, $\rho(t)$ is the reflection coefficient, and * denotes a convolution. In all practical cases the time $2t_0$ is longer than the step function rise time so that $V_{in}(t - 2t_0) = 1$. Finally, both displayed waveforms V_{sc} and V_0 are digitized and a discrete Fourier transform is calculated using a digital computer with the necessary corrections [3] in order to eliminate a large truncation error. The reflection coefficient can then be calculated by taking the ratio of both

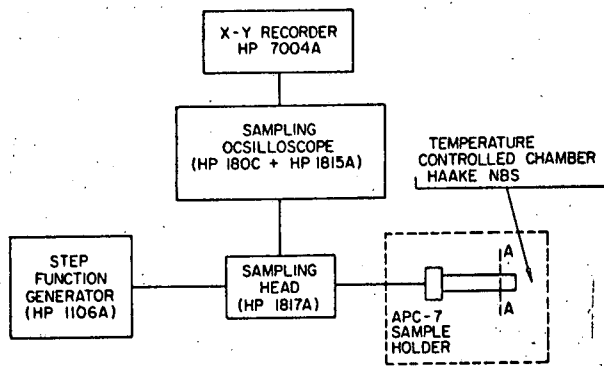


Fig. 2. Experimental setup.

discrete Fourier transforms, i.e.,

$$\begin{aligned} \rho(\omega) &= |\rho(\omega)| e^{-j\theta(\omega)} = \frac{FV_r(t-t_0)}{FV_{in}(t-t_0)} \\ &= \frac{F[V_{in}(t-t_0)*\rho(t)]}{FV_{in}(t-t_0)} \\ &= \frac{F[V_0(t) - V_{in}(t-2t_0)]}{-FV_{sc}(t-t_0)}. \end{aligned} \quad (12)$$

The frequency spectrum of the real and imaginary parts of the relative permittivity may hence be found from (8) and (9).

UNCERTAINTY ANALYSIS

In this section the total uncertainty in measurement of $\epsilon'_r(\omega)$ and $\epsilon''_r(\omega)$ resulting from the uncertainties in measurement of different quantities determining the permittivity of the test substance is discussed.

The final uncertainties in $\epsilon'_r(\omega)$ and $\epsilon''_r(\omega)$ are by definition expressed as

$$\Delta\epsilon' = \left(\left(\frac{\partial\epsilon'}{\partial C_0} \Delta C_0 \right)^2 + \left(\frac{\partial\epsilon'}{\partial Z_0} \Delta Z_0 \right)^2 + \left(\frac{\partial\epsilon'}{\partial \rho} \Delta \rho \right)^2 + \left(\frac{\partial\epsilon'}{\partial \theta} \Delta \theta \right)^2 \right)^{1/2} \quad (13)$$

$$\Delta\epsilon'' = \left(\left(\frac{\partial\epsilon''}{\partial C_0} \Delta C_0 \right)^2 + \left(\frac{\partial\epsilon''}{\partial Z_0} \Delta Z_0 \right)^2 + \left(\frac{\partial\epsilon''}{\partial \rho} \Delta \rho \right)^2 + \left(\frac{\partial\epsilon''}{\partial \theta} \Delta \theta \right)^2 \right)^{1/2} \quad (14)$$

where ΔC_0 , ΔZ_0 , $\Delta \rho$, and $\Delta \theta$ are the uncertainties in the air capacitance of the test capacitor, characteristic impedance of the transmission line, modulus, and phase of the reflection coefficient, respectively.

The partial derivatives appearing in (13) and (14) calculated from (8) and (9) are

$$\frac{\partial\epsilon'}{\partial C_0} = \frac{2\rho \sin \theta}{\omega C_0^2 Z_0 \{ (\rho \cos \theta + 1)^2 + \rho^2 \sin^2 \theta \}} \quad (15)$$

$$\frac{\partial\epsilon'}{\partial Z_0} = \frac{2\rho \sin \theta}{\omega C_0 Z_0^2 \{ (\rho \cos \theta + 1)^2 + \rho^2 \sin^2 \theta \}} \quad (16)$$

$$\frac{\partial\epsilon'}{\partial \rho} = \frac{2(1-\rho^2) \sin \theta}{\omega C_0 Z_0 \{ (\rho \cos \theta + 1)^2 + \rho^2 \sin^2 \theta \}^2} \quad (17)$$

$$\frac{\partial\epsilon'}{\partial \theta} = \frac{2\rho \{ (1+\rho^2) \cos \theta + 2\rho \}}{\omega C_0 Z_0 \{ (\rho \cos \theta + 1)^2 + \rho^2 \sin^2 \theta \}^2} \quad (18)$$

and

$$\frac{\partial\epsilon''}{\partial C_0} = -\frac{(1-\rho^2)}{\omega C_0^2 Z_0 \{ (\rho \cos \theta + 1)^2 + \rho^2 \sin^2 \theta \}} \quad (19)$$

$$\frac{\partial\epsilon''}{\partial Z_0} = -\frac{(1-\rho^2)}{\omega C_0 Z_0^2 \{ (\rho \cos \theta + 1)^2 + \rho^2 \sin^2 \theta \}} \quad (20)$$

$$\frac{\partial\epsilon''}{\partial \rho} = -\frac{2\{ 2\rho + (1+\rho^2) \cos \theta \}}{\omega C_0 Z_0 \{ (\rho \cos \theta + 1)^2 + \rho^2 \sin^2 \theta \}^2} \quad (21)$$

$$\frac{\partial\epsilon''}{\partial \theta} = \frac{2\rho(1-\rho^2) \sin \theta}{\omega C_0 Z_0 \{ (\rho \cos \theta + 1)^2 + \rho^2 \sin^2 \theta \}^2} \quad (22)$$

The uncertainties ΔC_0 and ΔZ_0 in (13) and (14) result from the uncertainties in length measurement and for the modern coaxial components can be assumed to be equal to 0.1 percent³ [4]. The uncertainties in $\Delta \rho$ and $\Delta \theta$ are, on the other hand, caused by the noise-like errors in the TDR system (in time domain) and by the time-to-frequency conversion errors.

A detailed analysis of different noise-like errors (quantization, amplitude jitter, time jitter, and white noise) and errors resulting from the time-to-frequency conversion (aliasing and truncation) as well as the bounds for these errors have been given in [3]. The results of this analysis have been utilized in calculations of the measurement uncertainty for the actual measurement setup in the reported experiments.

The numerical solutions of (13) and (14) (in the normalized form) for the typical values of the test capacitor $C_0 = 10$ pF and the characteristic impedance of the transmission line $Z_0 = 50 \Omega$ are presented in Figs. 3 and 4 as functions of $f\epsilon'_r$ and $f\epsilon''_r$ as a running parameter. The following uncertainties were assumed $\Delta C_0 = 3 \times 10^{-14}$ F (0.1 percent uncertainty in distance measurement), $\Delta Z_0 = 0.10 \Omega$ (typical for APC-7 coaxial connectors [4]) with $\Delta \rho = 1.40$ percent and $\Delta \theta = 0.8^\circ$ (maximum values calculated for the Hewlett-Packard TDR System consisting of the HP 180C oscilloscope, HP 1815 TDR plug-in, HP 1817A TDR sampler, and HP 1106A tunnel diode generator, for the frequency band 0.01-1.0 GHz using the formulas given in [3]).⁴

A detailed analysis of the uncertainties (13) and (14) shows that the most important is the uncertainty in the capacitance of the air-filled capacitor. Fortunately, this parameter can be determined with very high accuracy from the geometrical dimensions. A remaining major contribution comes from the uncertainties in the modulus and phase angle of the reflection coefficient. The uncertainties in ϵ'_r and ϵ''_r shown

³An additional uncertainty in the determination of C_0 results from the presence of the fringing field effects and the meniscus of the test liquid, but at the present stage it is very difficult to evaluate.

⁴An experimental verification of these calculations is now in progress.

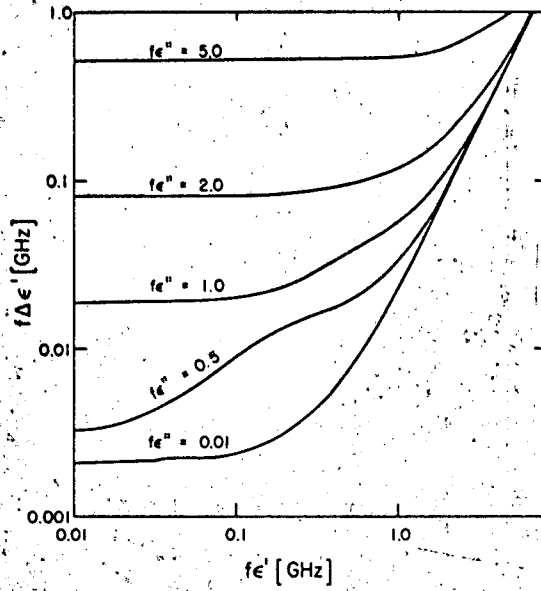


Fig. 3. Uncertainty in measurement of $f\epsilon'$ as a function of $f\epsilon'$ for different values of $f\epsilon''$.

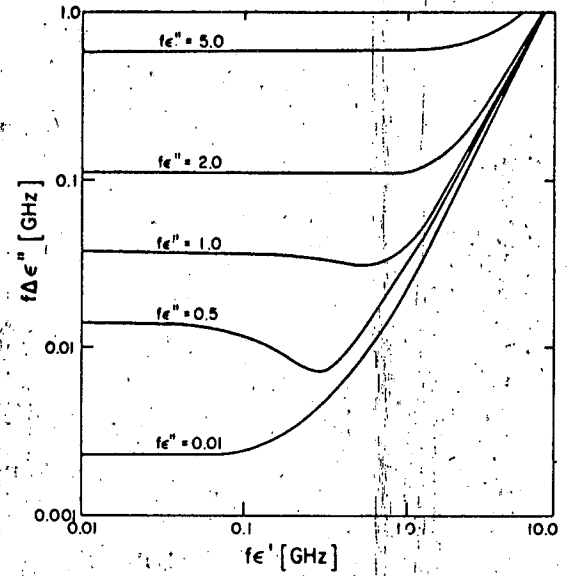


Fig. 4. Uncertainty in measurement of $f\epsilon''$ as a function of $f\epsilon'$ for different values of $f\epsilon''$.

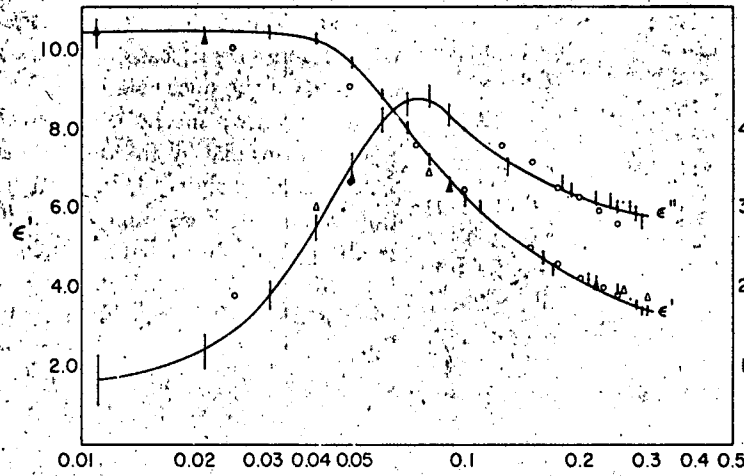


Fig. 5. Experimental results for the alkyl alcohol $C_8H_{17}OH$ at $16.5^\circ C$. Δ -points calculated based on data given in [4] assuming the ideal Debye dispersion with the single relaxation time. \circ -experimental points from [6]. Horizontal scale: Frequency in gigahertz.

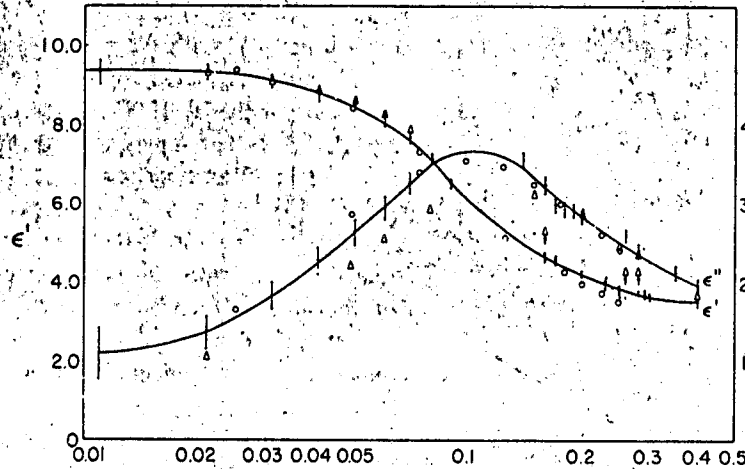


Fig. 6. Experimental results for the alkyl alcohol $C_8H_{17}OH$ at $25^\circ C$. Δ -points calculated based on data given in [4] assuming the ideal Debye dispersion with the single relaxation time. \circ -experimental points from [6]. Horizontal scale: Frequency in gigahertz.

in Figs. 5 and 6 have been calculated for the given frequency band, as a sum of the absolute values of maximum possible errors in ϵ' and ϵ'' , caused by the errors in the modulus and phase of the reflection coefficient occurring simultaneously.

Further analysis of (13) and (14) shows that the major frequency band limitation of the time domain method is related to the capacitance of the air-filled capacitor. Large capacitances give smaller uncertainties at lower frequencies and, vice versa, small capacitances are better at higher frequencies. A compromise is usually required for any given frequency band. Additional high-frequency limitation of this technique is due to the noise of the measuring system that becomes especially pronounced at higher frequencies as a result of the limited spectral density of the incident step.

EXPERIMENTAL RESULTS

Feasibility of the method was evaluated experimentally by measurements of the dielectric properties of some alkyl alcohol, which have been studied by several authors in frequency domain [6].

The size of the sample was basically determined by the gap between the inner conductor of the sample holder and the terminating metal plate as well as by the viscosity of the liquid. In the reported experiments the sample holder was kept in the vertical position in order to avoid spilling of the test sample, although any liquid film present on the terminating plate has negligible effect on the system response, due to the fact that the electric field at this surface is also negligibly small.

The experimental results shown in Figs. 5 and 6 are generally in good agreement with the data obtained by the frequency domain methods in [6] (circles in Figs. 5 and 6). Relatively larger differences are observed between the experimental results in the time domain and the values of ϵ' and ϵ'' calculated⁵ from the data in [4] (triangles in Fig. 5 and 6). This is

⁵Values of ϵ' and ϵ'' were calculated assuming the Debye dispersion with single relaxation time.

probably due to the large uncertainty in the determination of τ as suggested in [7], [8].

CONCLUSION

A novel technique for measurements of the dielectric properties of biological substances in time domain, which utilizes a small shunt capacitor terminating a coaxial line section as a sample holder, has been described. This technique gives all necessary information on the frequency behavior of the tested substance, while the required sample volume is of the order of a few cubic millimeters. The greatest assets of the proposed method are its speed, simplicity, relative ease of data evaluation, and very small sample requirement. The display on the oscilloscope screen gives immediate information about the behavior of the investigated sample in a very broad frequency range that is limited at both ends by the capacitance of the test capacitor C_0 and at the upper end also by the rise time of the system.

ACKNOWLEDGMENT

The authors wish to acknowledge the effort of J. Putnam for his assistance in manufacturing the test capacitor.

REFERENCES

- [1] H. P. Schwan, "Application of UHF impedance measuring techniques in biophysics," *IRE Trans. Instrum.*, vol. PG-4, pp. 75-83, Oct. 1955.
- [2] A. M. Nicolson and G. F. Ross, "Measurement of the intrinsic properties by time-domain technique," *IEEE Trans. Instrum. Meas.*, vol. IM-19, pp. 377-382, Nov. 1970.
- [3] G. F. Ross *et al.*, "Transient behaviour of microwave networks," Sperry Rand, Res. Rep. SRRR-CR-68-2, 1968.
- [4] H. Fellner-Fedlegg, "The measurement of dielectrics in the time domain," *J. Phys. Chem.*, vol. 73, pp. 616-623, Mar. 1969.
- [5] M. F. Iskander and S. S. Stuchly, "Time domain response for dielectrics showing the Debye dispersion with distributed relaxation times," *Instrum. Meas.*, to be published.
- [6] S. K. Garg and C. P. Smyth, "Microwave absorption and molecular structure in liquids LXII. The three dielectric dispersion regions of the normal primary alcohols," *J. Phys. Chem.*, vol. 69, no. 4, pp. 1294-1301, 1965.
- [7] T. A. Whittingham, *J. Phys. Chem.*, vol. 73, p. 616, 1969.
- [8] H. Fellner-Fedlegg and E. F. Barnett, *J. Phys. Chem.*, vol. 74, pp. 1962-1965, 1970.